Supporting Information

Activating paddle-wheel effects towards lower temperature in a new sodium-ion solid electrolyte, $Na_{3.5}Si_{0.5}P_{0.5}Se_4$

Yu Yang[a], Zhenming Xu[b], Chaohong Guan[a], Runxin Ouyang[a], Huirong Jing[a], Hong Zhu[a*]

[a]University of Michigan−Shanghai Jiao Tong University Joint Institute, Shanghai Jiao Tong University, 800, Dongchuan Road, Shanghai 200240, China.

[b]College of Materials Science and Technology, Nanjing University of Aeronautics and Astronautics, Nanjing 210016, China.

*E-mail: hong.zhu@sjtu.edu.cn.

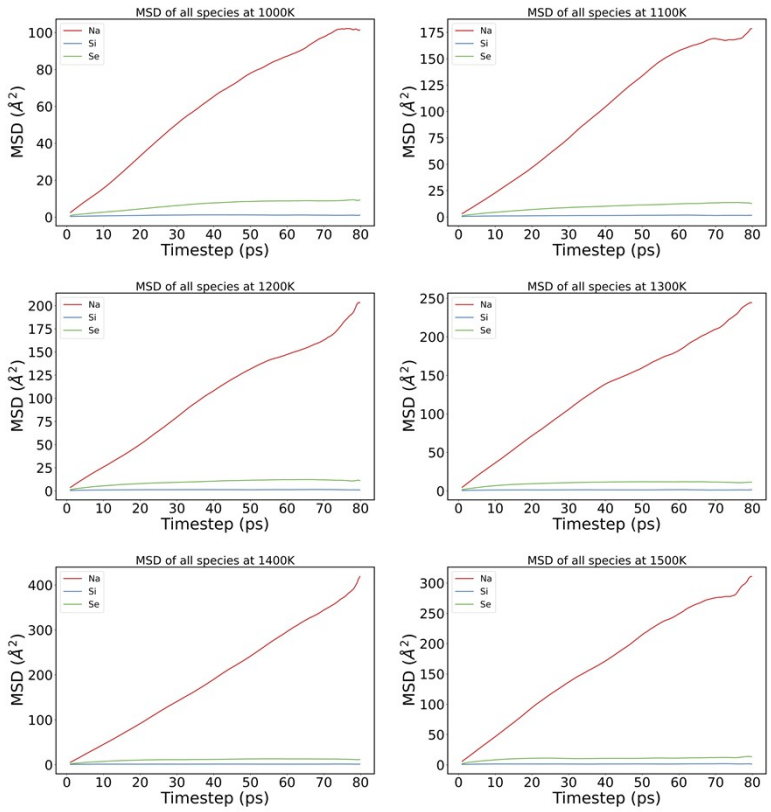

Figure S1. The species projected MSD plots of Na_4SiSe_4. The maximum value of the Si MSD is less than 3 $Å^2$ and the maximum value of the Se MSD is less than 10 $Å^2$.

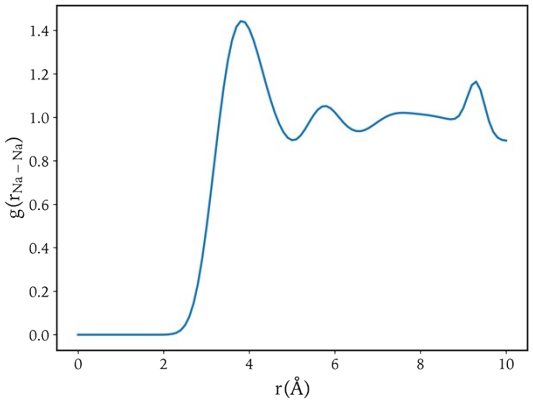

Figure S2. Na-Na radial distribution function of Na_4SiSe_4 at 1000 K. The first peak at ~3.8 Å, which equals the average distance between neighbor Na sites in Na_4SiSe_4.

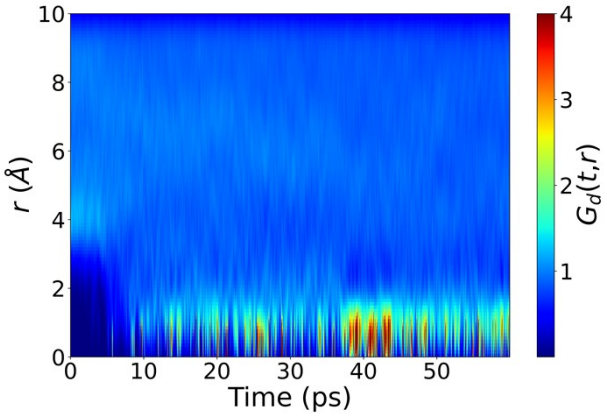

Figure S3. Plots of the distinct-part of the van Hove correlation function (G_d) for Na_4SiSe_4 at 1000 K. G_d is a function of the Na-Na pair distance r and time t.

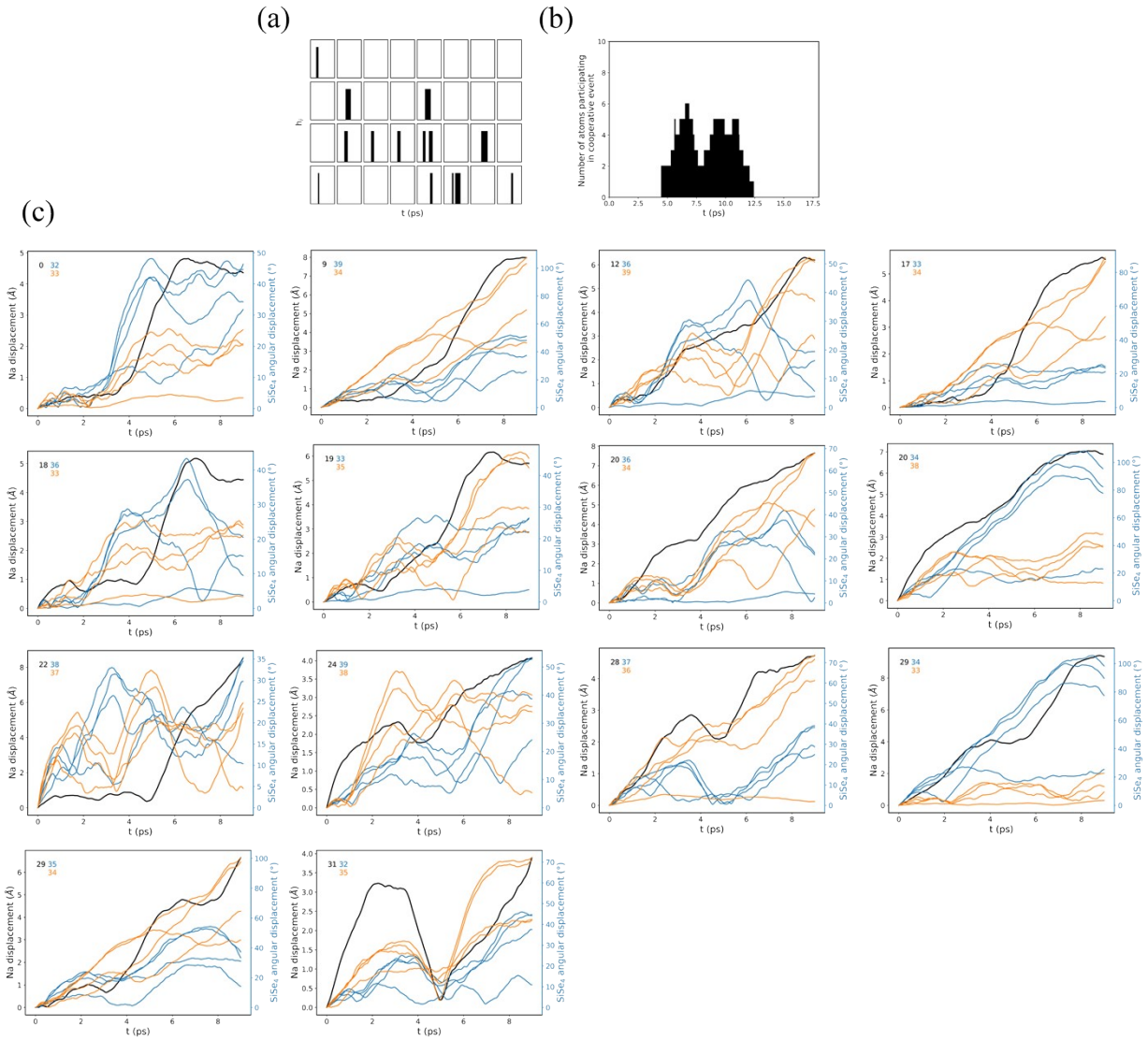

Figure S4. Characterization of Na migration events, and their correlation with rotational displacements of $SiSe_4$ polyanion, in Na_4SiSe_4 during the second 20 ps trajectory at 1000 K. (a) Identification of individual Na-ion migration events. (b) Number of Na atoms participating in the cooperative migration event as a function of the time which those events were observed. (c) Displacements of Na-ions (black line, left axis) that participate in the migration events identified in (a), and the angular displacements of the two nearest-neighbor $SiSe_4$ anions (blue and orange line, right axis). The ID for each Na and $SiSe_4$ polyanion is marked in the top left corner of each plot. Four rotational displacements are plotted for each $SiSe_4$ polyanion using same color, corresponding to the rotation of the four Se atoms around the center of mass of the $SiSe_4$ polyanion. To identify long-lived Na displacements more clearly (to differentiate from local vibrations), The atom positions in (d) are averaged over a moving time window of width equal to 2 ps.

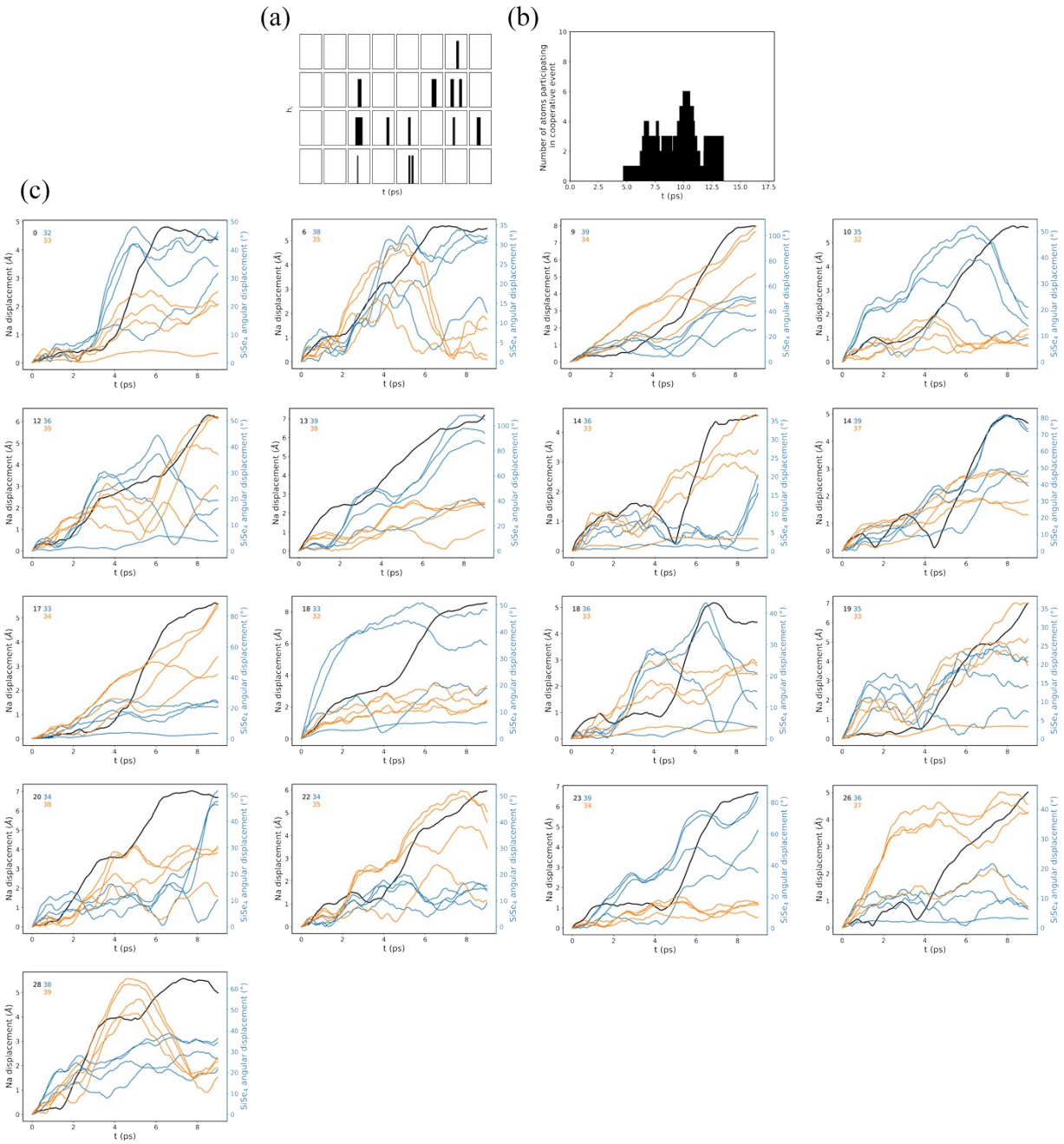

Figure S5. Characterization of Na migration events, and their correlation with rotational displacements of $SiSe_4$ polyanion, in Na_4SiSe_4 during the third 20 ps trajectory at 1000 K. See the caption of Figure S4 for additional details.

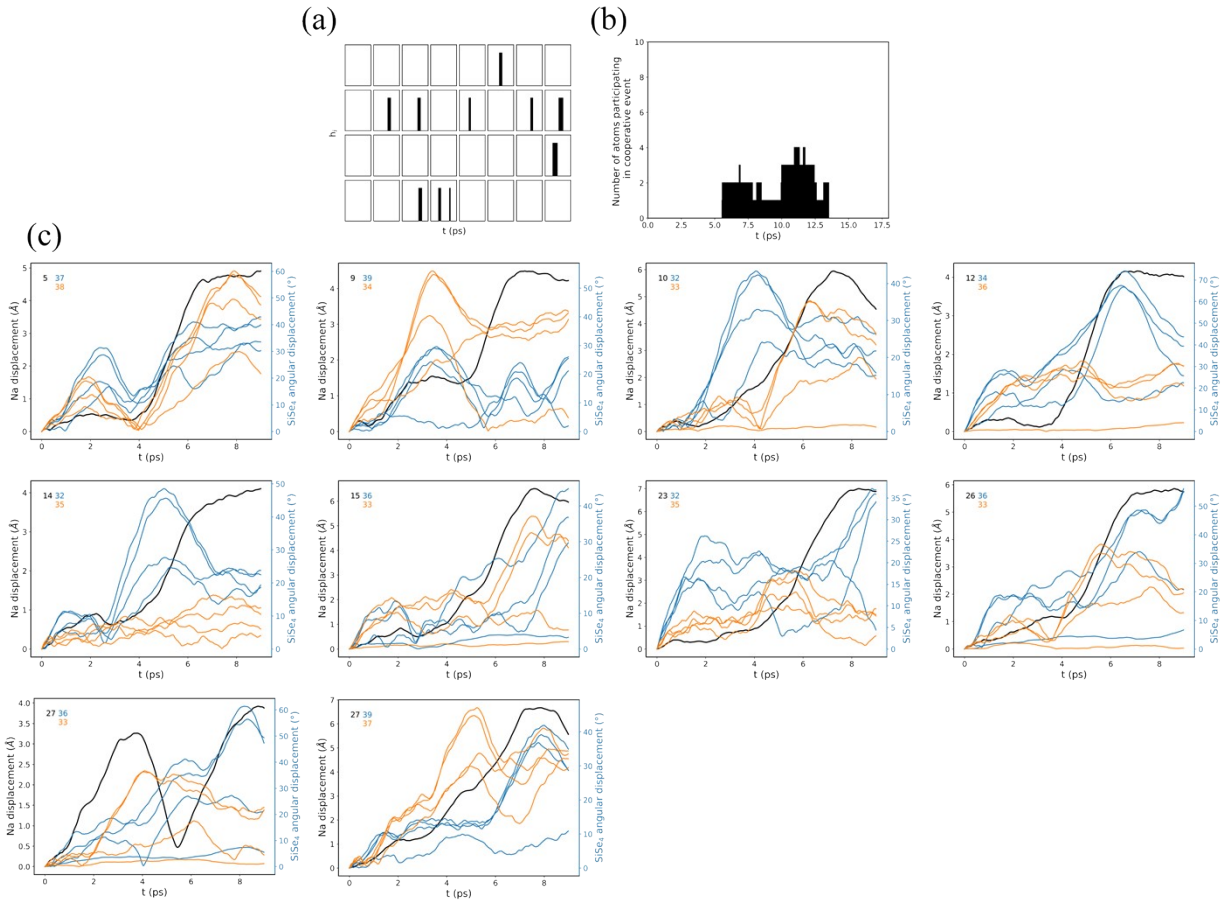

Figure S6. Characterization of Na migration events, and their correlation with rotational displacements of $SiSe_4$ polyanion, in Na_4SiSe_4 during the fourth 20 ps trajectory at 1000 K. See the caption of Figure S4 for additional details.

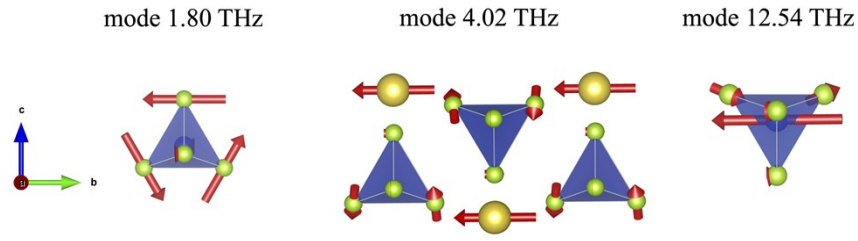

Figure S7. Typical vibrational modes were obtained by processing the eigenvalues of phonon calculations. Na, Si, and Se are labelled as yellow, bule, and green spheres, respectively.

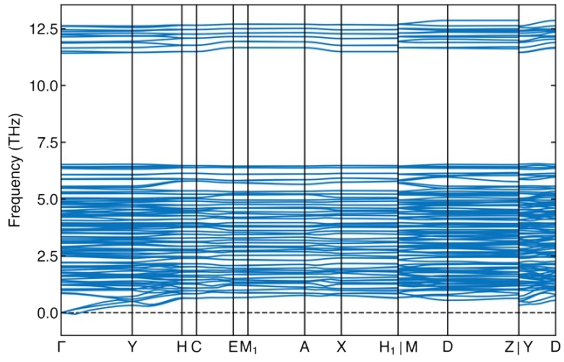

Figure S8. Calculated phonon dispersions of $Na_{3.5}Si_{0.5}P_{0.5}Se_4$.

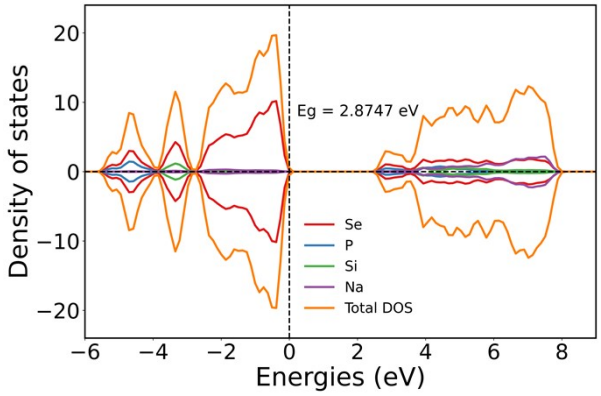

Figure S9. Density of states and band gap (E_g) of $Na_{3.5}Si_{0.5}P_{0.5}Se_4$.

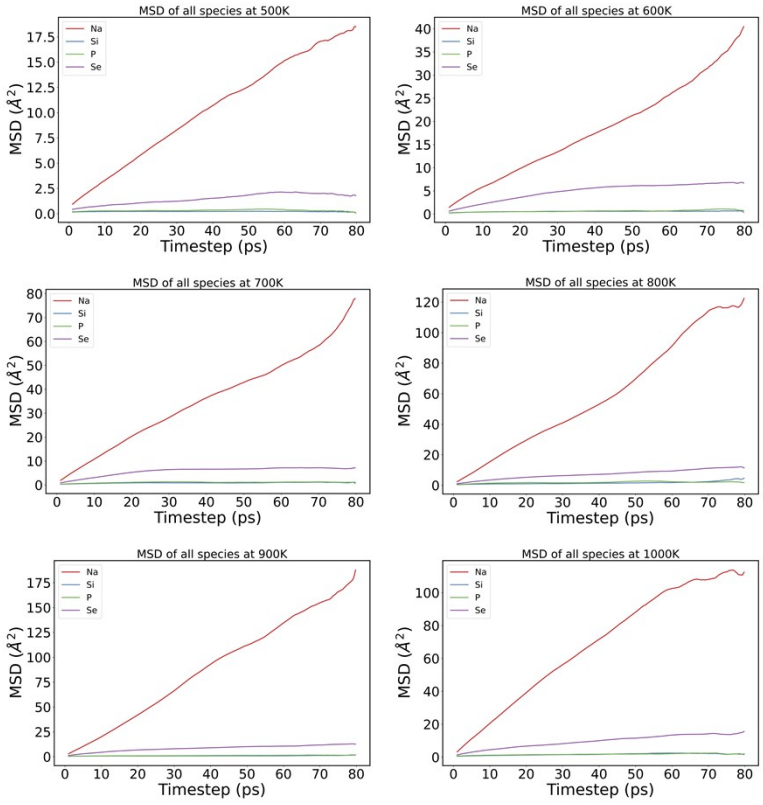

Figure S10. The species projected MSD plots of $Na_{3.5}Si_{0.5}P_{0.5}Se_4$.

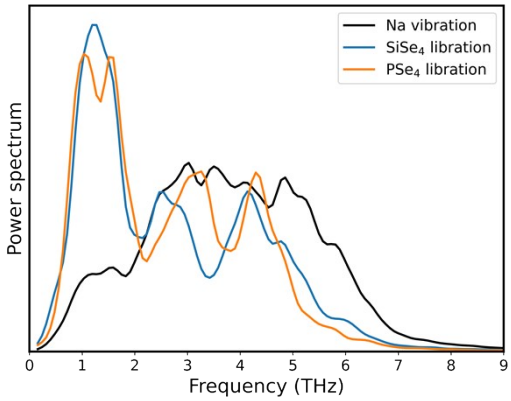

Figure S11. Power spectrum calculated via the Fourier transform of linear velocity autocorrelation for Na (black) and angular velocity autocorrelation for $SiSe_4$ (blue) and PSe4 (orange) at 300 K in $Na_{3.5}Si_{0.5}P_{0.5}Se_4$.

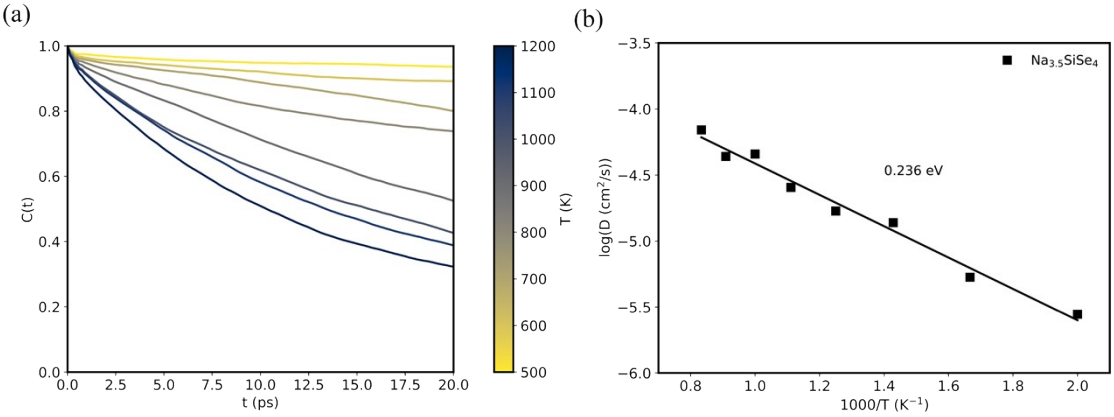

Figure S12. (a) Reorientation autocorrelation function $C(t)$ for $SiSe_4$ as a function of temperature in $Na_{3.5}SiSe_4$. (b) Calculated diffusivities and activation energies using the Einstein formula for $Na_{3.5}SiSe_4$.

Table S1. Structural information of Na_4SiSe_4.

a/Å	b/Å	c/Å
7.22	9.28	14.54
α	β	γ
90°	90°	90°

Table S2. Structural information of $Na_{3.5}Si_{0.5}P_{0.5}Se_4$.

a/Å	b/Å	c/Å
7.23	9.56	13.86
α	β	γ
90°	85.5°	90°

Table S3. Average atomic Bader charges (e) in $Na_{3.5}Si_{0.5}P_{0.5}Se_4$.

Species	Bader charge (e)
Na	0.84
Si	1.81
P	0.40
Se (ligand is Si)	−1.29
Se (ligand is P)	−0.74

Table S4. Calculated room temperature ionic conductivity, activation energy and the coefficient of determination (R^2) of Arrhenius plot for Na_4SiSe_4 and $Na_{3.5}Si_{0.5}P_{0.5}Se_4$. The calculated data of $Na_{11}Sn_2PS_{12}$ (ref. 1), $Na_7P_3S_{11}$ (ref. 2) and $Na_{2.875}PS_{3.875}Cl_{0.125}$ (ref. 3) were also listed for comparison.

Composition	σ_{300K} (mS/cm)	E_a (eV)	R^2
Na_4SiSe_4	1.42	0.279	0.88
$Na_{3.5}Si_{0.5}P_{0.5}Se_4$	16.94	0.195	0.94
$Na_{11}Sn_2PS_{12}$	2.77	0.243	—
$Na_7P_3S_{11}$	10.97	0.217	—
$Na_{2.875}PS_{3.875}Cl_{0.125}$	6.38	0.199	—

Note. — denotes the coefficient of determination is not calculated in the reference.

References

[1] Zhu, Z., Tang, H., Qi, J., Li, X. G., & Ong, S. P. (2021). Design Principles for Cation‐Mixed Sodium Solid Electrolytes. Advanced Energy Materials, 11(7), 2003196.

[2] Wang, Y., Richards, W. D., Bo, S. H., Miara, L. J., & Ceder, G. (2017). Computational prediction and evaluation of solid-state sodium superionic conductors Na7P3X11 (X= O, S, Se). Chemistry of Materials, 29(17), 7475-7482.

[3] Feng, X., Chien, P. H., Zhu, Z., Chu, I. H., Wang, P., Immediato‐Scuotto, M., ... & Hu, Y. Y. (2019). Studies of Functional Defects for Fast Na‐Ion Conduction in Na3− yPS4− xClx with a Combined Experimental and Computational Approach. Advanced Functional Materials, 29(9), 1807951.